Quantitative XANES Studies on Metastable Equilibrium Adsorption of Arsenate on TiO_2 Surfaces

Guangzhi He,[†] Gang Pan,*[,†] Meiyi Zhang,[†] and Ziyu Wu[‡]

State Key Laboratory of Environmental Aquatic Chemistry, Research Center for Eco-Environmental Sciences, Chinese Academy of Sciences, Beijing 100085, China, and National Synchrotron Radiation Laboratory, University of Science and Technology of China, Hefei, Anhui 230026, China

Received: May 14, 2009; Revised Manuscript Received: August 2, 2009

Quantitative information on the electronic and geometric structures of adsorption complexes of arsenate on TiO_2 surfaces was obtained on the basis of XANES analysis combined with DFT calculation. The density of states (DOS) showed that the As(V) K-absorption edge corresponded to the dipole transition from the As 1s electron into the As(4p)−O(2p) antibonding molecular orbital, suggesting that the bonding between arsenate and TiO_2 was primarily due to the interaction of As 4p and O 2p orbitals. Previous EXAFS studies indicated that both bidentate binuclear (BB) and monodentate mononuclear (MM) surface complexes coexisted in the As(V)−TiO_2 adsorption system. DFT calculation showed that the XANES transition energy of the BB complex was significantly higher than that of the MM complex. Thus, quantitative information on adsorption microstructures can be obtained by measuring the blue-shift of the XANES absorption edge. XANES results of adsorption samples at different kinetic stages indicated that there was a structural evolution from the MM complex to the BB complex as the reaction processed to adsorption equilibrium. Therefore, the final proportion between BB and MM complexes in the real equilibrium state was fundamentally affected by surface coverage and kinetic pathways. This fact implied that the real equilibrium constant, when defined by macroscopic parameters of concentration and adsorption density (mol/m^2), are generally inconstant in nature and hence cannot describe the real equilibrium properties of adsorption, because different microscopic metastable equilibrium adsorption structures that construct the real adsorption equilibrium cannot be counted for both mass and energy by the macroscopic parameter of surface concentrations (mol/m^2).

1. Introduction

X-ray absorption near edge structure (XANES) directly probes the unoccupied density of states (DOS) and gives information on the electronic distribution and local geometry of the absorber.[1,2] XANES has high sensitivity to interactions between the absorber and its coordination environment, which is 10−20-fold greater than that of EXAFS (extended X-ray absorption fine structure).[3,4] The advantage of sensitivity allows XANES spectra to be potentially effective for detecting the slight difference between adsorption samples (e.g., from the same adsorption system but during different kinetic pathways) and a low concentration sample that is difficult for EXAFS measurement. XANES presents three-dimensional information for multiple scattering paths, while EXAFS only gives one-dimensional information for single scattering. Therefore, XANES can provide additional information in analyzing surface topology.[4] However, current applications of XANES are mostly empirical in nature, which has greatly limited its usage. If it can be quantified, XANES analysis methods can be used to explore the relationship between electronic structures and local geometry of absorber that is hidden in XANES spectra. Such a method will provide substantial experimental insights in surface adsorption mechanisms at the solid−liquid interface.

The authors have systematically studied the metastable equilibrium adsorption (MEA) behavior using thermodynamic experiments, EXAFS, IR spectroscopy, and DFT calculation.[5−7] However, previous studies using these experimental and theoretical methods are largely restricted to identifying the geometry of the final adsorption states.[8−11] There is little investigation on the density of states (DOS) of adsorbate before, after, and during the adsorption processes. The influence of surface adsorption on electronic structure of adsorbate and the geometric information hidden in electronic states have not been experimentally studied because of the limitation in technologies. In aspect of thermodynamics, a new phenomenon called initial concentration effect (i.e., C_0 effect) was observed in the As(V)−TiO_2 adsorption system, where, under the same thermodynamic condition, the equilibrium adsorption isotherm was fundamentally affected by kinetic pathways (one batch or multi-batch addition of arsenate).[7] The existence of the C_0 effect implied that the real equilibrium constant, when defined by macroscopic parameters of concentration and adsorption density, was affected by not only thermodynamic conditions but also adsorption kinetics. Experimentally measured equilibrium adsorption constants therefore bear the property of inconstancy in nature. Previous EXAFS explanation of the C_0 effect was limited to the geometric analysis of MEA states.[5,7] Quantitative analysis of electronic states on the mechanism of C_0 effect using experimental XANES has never been reported before.

Here, adsorption samples of arsenate on TiO_2 surfaces at different kinetic stages were measured using XANES. DFT molecular orbital calculation was used to get the theoretical XANES transition energy of each dominant Ti−AsO_4 surface complex. Then, the calculated results were applied to experi-

* Corresponding author. Phone: +86-10-62849686. Fax: +86-10-62923541. E-mail: gpan@rcees.ac.cn.
[†] Chinese Academy of Sciences.
[‡] University of Science and Technology of China.

10.1021/jp9044918 CCC: $40.75
Published on Web 09/09/2009

mental XANES spectra to extract quantitative structural information based on the blue-shift of the XANES absorption edge. Structural evolution of surface complexes during the kinetic process and the mechanism of the C_0 effect were studied using XANES analysis. The method provided direct evidence on what different MEA states coexisted under a fixed thermodynamic condition for a given adsorption reaction and how the real equilibrium state was affected by kinetic pathways.

2. Theoretical and Experimental Methods

2.1. Theoretical Section. ***2.1.1. XANES Simulation.*** As(V) K-edge theoretical XANES spectra and DOS were calculated using full multiple scattering (FMS) theory (i.e., all scattering paths were summed within a specified cluster volume[12]) and the ab initio self-consistent field potential model by FEFF8.2 code. DOS denotes the contribution of an atomic orbital to a molecular orbital. The greater the DOS, the greater the probability of electron transition into a corresponding antibonding molecular orbital.[1] The self-consistent field potential model is more accurate for XANES and DOS calculation than atomic overlap Mattheiss prescription, because the former takes the charge transfer into account and is more reliable in estimating the Fermi level.[13] The Hedin−Lundqvist exchange correlation potential was used with a muffin-tin radii overlap of 15%. A core hole was included in order to imitate the final state of the photon absorption process. Each type of scatterer (i.e., neighbor O and Ti atoms) was calculated with unique potentials. Proton effect was demonstrated to be insignificant in the test calculation, so the protons were neglected in the final calculation.

For the XANES simulation, a ~8.5 Å radius Ti−AsO_4 surface cluster (typically ~160 atoms) was employed, in which convergence had occurred. The geometries of arsenic and the first-neighbor oxygen atoms were optimized using DFT calculation, and the substrate kept the structure of anatase TiO_2(100) surface, which is one of the dominant lattice planes in the natural anatase mineral.[14,15]

2.1.2. DFT Calculation. It was reported that the surface of anatase TiO_2 particle predominantly consists of (101), (100) and (001) crystal planes,[14,15] and the exposition of the crystal plane depends on the synthetic technique.[16,17] In a related study,[6] we selected a Ti_2O_8 cluster of (100) surface for DFT calculation. The good agreement of calculated As−O and As−Ti distances with experimental EXAFS results indicates that (100) surface is dominant in the TiO_2 powder used in our adsorption experiment. There are two different oxygens, O(2) and O(3), in anatase TiO_2, which were bonded by two and three titanium atoms, respectively.[16] To eliminate the boundary effect and reduce the charge of clusters, the eight boundary oxygens in the Ti_2O_8 model cluster were saturated with 12 H atoms to ensure the bonding numbers of O(2) and O(3) were same as that of the anatase bulk structure.[11,18−21] Therefore, a $[Ti_2(OH)_4(H_2O)_4]^{4+}$ surface cluster of TiO_2 was used in this calculation.

For arsenate, $H_2AsO_4^-$ is the most dominant species at pH 7.0.[10,11] Thus, $H_2AsO_4^-$ species was used in DFT calculation. In a related study,[6] the chemical reactivity analysis of arsenate ($H_2AsO_4^-$) and TiO_2 showed that inner-sphere complexation occurred via ligand exchange of the two unprotonated oxygen atoms on arsenate with TiO_2 surface hydroxy groups. Therefore, $Ti_2(OH)_4(H_2O)_4AsO_2(OH)_2^{3+}$ and $Ti_2(OH)_5(H_2O)_4AsO_2(OH)_2^{2+}$ adsorption clusters were used to determine the geometry and molecular orbital energy of Ti−AsO_4 surface complexes. Previous EXAFS and DFT studies proved that bidentate binuclear (BB) and monodentate mononuclear (MM) were two dominant adsorption complexes of arsenate on TiO_2 surfaces.[6] To avoid over-relaxation of the cluster model,[10,18,20] low-spin and restricted closed-shell DFT-B3LYP calculation formalism and substrate-fixed strategy were employed. The DFT-B3LYP approach is a generalized gradient approximation (GGA) method and has been widely used to study adsorption of oxyanions on transition metal oxides.[10,22,23] The geometry and molecular orbital energy were predicted using the 6-31+G(d) basis set on O and H, the 6-311+G(d) basis set on As, and the LANL2DZ relativistic effective core potential (RECP) basis set on Ti atoms. The LANL2DZ basis set was used because it took the relativistic effect into account, which was necessary for transition metals.[18,24] The DFT calculation was performed using Gaussian 03.[22]

2.2. Experimental Section. ***2.2.1. XANES Samples Preparation.*** In order to study the mechanism of initial concentration (C_0) effect and how the real equilibrium adsorption states were affected by reaction kinetic pathways, adsorption samples of multi-batch isotherm and kinetic experiments were collected and subjected to XANES analysis.

Two comparable adsorption samples (A_1 and A_2) from one-batch and three-batch isotherms were chosen for XANES measurement to see how the electronic state and microstructure of the adsorbed arsenate are different in these samples. The two samples were generated from the same initial condition (0.80 mmol/L total arsenate and 1.0 g/L TiO_2 particle) but ended in different "equilibrium" states when the reactions were completed through one-batch and three-batch pathways (see Figure 1 in ref 7).

In a conventional one-batch isotherm experiment, the initial arsenate (0.80 mmol/L) was added once to the suspension of TiO_2 (1.0 g/L, 30 mL), and the polypropylene centrifuge tubes were capped and shaken for 24 h. In the three-batch isotherm experiment, the total mass of arsenate (0.80 mmol/L) was equally divided into three parts and each part was added to the same reaction tube containing TiO_2 suspension (1.0 g/L, 30 mL) every 4 h and then shaken for 16 h (total reaction time was 24 h), where the total mass and the thermodynamic conditions for each tube remained the same as those in the one-batch isotherm experiment. The adsorption experiments were conducted in 0.01 M $NaNO_3$ solution at 25 °C. The pH of the reaction system was constantly monitored and adjusted to the desired value of 7.0 with 0.1 mol/L NaOH or 0.1 mol/L HNO_3. Kinetic experiments indicated that adsorption reached an apparent equilibrium within 4 h (see Figure 2 in ref 7). The isotherm samples were equilibrated for 24 h. After 24 h of equilibration, suspensions of one- and three-batch adsorption experiments were centrifuged and then filtered through 0.25 μm nominal pore size membrane filters prior to analysis. The moist solids of adsorption samples were mounted in a 2-mm-thick cell and sealed with adhesive PVC tape for XAFS measurements.

A conventional adsorption kinetic experiment (one-batch) was conducted by adding the total mass of arsenate (0.57 mmol/L) into 1.0 g/L TiO_2 suspension in 1-L glass conical flasks once, and then three samples were collected at 5 min (A_3), 4 h (A_4), and 11 h (A_5) after the total arsenate addition. A multi-batch kinetic experiment (three-batch) was conducted by dividing the total arsenate of 0.57 mmol/L into three equal parts and adding them into the reaction vessel in succession at 0, 4, and 8 h and then taking aliquots of samples at different times to monitor the kinetic process. During the multi-batch kinetic process, four samples were collected at 5 min (A_6, A_8) and 4 h (A_7, A_9) after the first two additions of arsenate, and two samples were collected at 5 min (A_{10}) and 13 h (A_{11}) after the third addition.

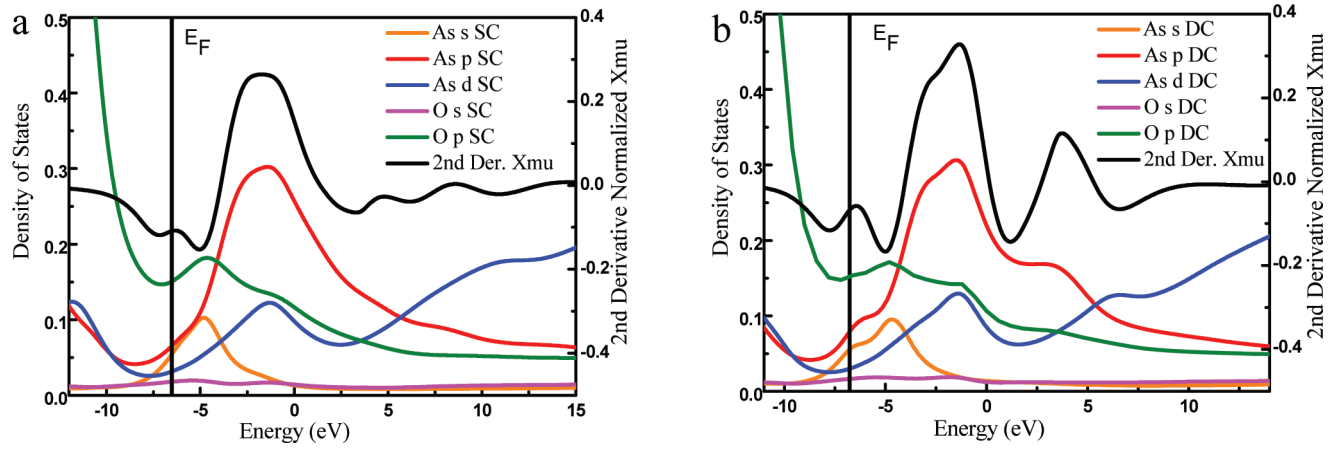

Figure 1. The electron DOS and the negative second derivative XANES spectra of (a) MM and (b) BB Ti−AsO_4 surface complexes calculated using FEFF8.2 code. The Fermi level was calculated to be ca. −6.6 eV.

XANES sample numbers are clearly shown in Figures 1 and 2 in ref 7. The suspension of one- and three-batch kinetic experiments was stirred with a magnetic stirrer and pH was maintained at 7.0 by adding 0.1 mol/L NaOH or 0.1 mol/L HNO_3.

Desorption experiments were conducted by removing the equilibrium supernatant after centrifugation, replacing the solution with an equal volume of 0.01 mol/L $NaNO_3$ background solution, adjusting the pH to 7.0, and then shaking the mixture for 24 h. Other analytical procedures were the same as described above. The desorption process was repeated two times to get a desorption sample.[25] The desorption samples marked by "D" were measured to study the adsorption irreversibility. All the adsorption and desorption experiments were in 0.01 mol/L $NaNO_3$ solution at 25 °C and pH 7.0. The operation of adsorption/desorption experiments and the preparation of samples were described in detail in a related thermodynamic and EXAFS study.[7] All reagents used in this study were analytical grade, and labware was acid-washed.

2.2.2. XANES Data Collection. As(V) K-edge XANES data were collected on beamline 4W1B at Beijing Synchrotron Radiation Facility (BSRF), China. Spectra for two arsenate solution samples and all adsorption samples were collected under ambient conditions using a 0.05 eV step size in the range from −5 to 5 eV of the absorption edge to resolve absorption edge features. The spectra of solid-phase samples were collected in fluorescence mode because As(V) concentration was low in adsorption samples, and the standard reference As(V) aqueous solutions ($Na_2AsO_4 \cdot 7H_2O$) were measured in transmission mode. An average of three scans was performed to achieve an adequate signal/noise ratio. Background subtraction and normalization of all experimental spectra were achieved with the WinXAS3.1 software package.[26] To remove the background absorbance, spectra were background-corrected using a two-polynomial fit. Following the background correction, sample spectra were normalized.

3. Results and Discussion

3.1. Density of States. The DOS and negative second derivative of calculated XANES spectra of MM and BB Ti−AsO_4 surface complexes are presented in Figure 1. Absorption edge positions were determined by the peak of the second derivative of the calculated XANES. The Fermi level E_F was determined by self-consistent field calculation. The occupied molecular orbitals were those below E_F and the antibonding molecular orbitals were those above E_F. The comparison between the absorption edge position and valence orbital density for MM (Figure 1a) and BB (Figure 1b) surface complexes indicated that the XANES absorption edge was primarily due to the dipole transition from the As 1s electron into the As(4p)−O(2p) antibonding molecular orbital.

The arsenic 4p orbital and oxygen 2p orbital showed a good symmetry match due to their p-orbital character, where the p-orbital localized along the As−O bond vector and formed strong bonding and antibonding. The stronger the bonding interaction, the higher antibonding energy and destabilization of antibonding orbital and hence the greater transition probability.[1] Therefore, the transition probability of the As 1s electron into the As(4p)−O(2p) antibonding orbital was greater than any other antibonding orbitals. None of occupied states (e.g., core electrons, Ti−O and As−O bonding orbitals, oxygen lone pairs) directly contributed to XANES spectra. Model clusters used in XANES simulation are shown in Figure 2.

3.2. XANES Transition Energy Calculated by DFT. A schematic diagram of the molecular orbital energy order and electronic transition level of MM and BB geometries was obtained by DFT calculation (Figure 3). The sequence of orbital energy indicated that the theoretical XANES transition energy from the As(1s) orbital into the As(4p)−O(2p) antibonding molecular orbital of BB complex was 0.62 eV higher than that of MM complex.

DFT-calculated geometries of MM and BB Ti−AsO_4 surface complexes are shown in Figure 4a,b. In the MM surface complex, arsenate bonded on TiO_2 surfaces by only one chemical bond at a As−O distance of 1.74 Å (Figure 4a). In the BB surface complex, arsenate bonded to TiO_2 surfaces by two bonds at As−O distances of 1.71 Å (Figure 4b), where the electron density between As and O and hence the As−O bonding and antibonding interaction were enhanced versus that of the MM surface complex. The strong interaction of As−O bonds in BB complex resulted in higher As(4p)−O(2p) antibonding energy than that in the MM complex, which consequently led to the difference in XANES spectral features, namely, the absorption edge of BB complex was 0.62 eV higher than that of the MM complex (Figure 3).

3.3. XANES Evidence of Structural Evolution of Surface Complexes. The first-derivative XANES spectra showed that the absorption edge shifted from low to high energy in the order of $A_1 < A_2 < D_1 < D_2$. However, no shift was observed for the two arsenate solutions (pH 5.5 and 7.0) (Figure 5), suggesting that the shift of XANES absorption edge was due to surface complexation rather than protonation effect.

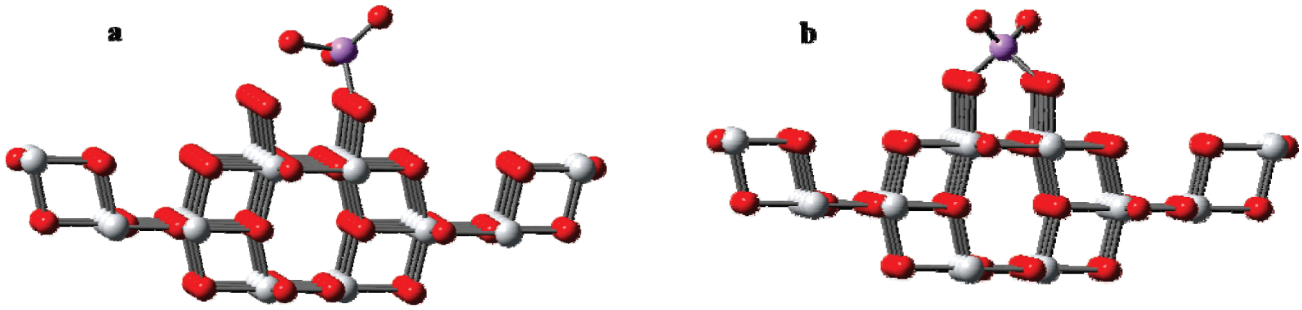

Figure 2. Clusters of As(V) bond on anatase TiO_2(100) surface used in XANES calculations: (a) monodentate mononuclear structure and (b) bidentate binuclear structure. Purple, red, and gray circles denote As, O, and Ti atoms, respectively.

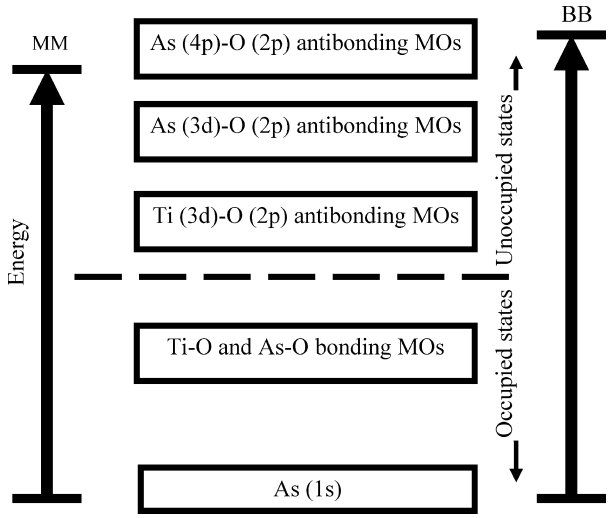

Figure 3. Schematic diagrams of molecular orbitals and electron transition for Ti−AsO4 surface complexes in MM and BB bonding mode.

For isotherm samples, the absorption edge energy increased by 0.16 eV from one-batch (A_1) to three-batch (A_2) adsorption samples (Figure 5). On the basis of Figure 3, where the XANES absorption edge of BB complex was 0.62 eV higher than that of MM complex, the blue-shift of the absorption edge from one- to three-batch equilibrium adsorption sample indicated the increase of BB complex in the three-batch adsorption experiment. The blue-shift of absorption edge was also observed in desorption processes ($A_1 < D_1$ and $A_2 < D_2$), indicating that more MM adsorbed arsenate was desorbed than that of BB during the desorption process.

For one-batch adsorption kinetics, the absorption edge of the sample collected at 4 h after the total arsenate addition (A_4) was 0.20 eV higher than that collected at 5 min (A_3), and the energy shift was flatten off after 4 h (Figure 6a), indicating that there was a structural transform from MM to BB adsorption mode as the reaction processed to equilibrium. For three-batch kinetic samples, the total blue-shift observed in the absorption edge from A_6 to A_{11} was 0.42 eV (Figure 6b), which confirmed again that the multi-batch experiment was more favorable to the evolution from MM to BB complex than the conventional one-batch experiment. The extent of transform from MM to BB was affected by kinetic pathway (one-batch and multi-batch kinetic modes), indicating that the real "equilibrium" adsorption state on the solid surface was not only determined by thermodynamic condition but also controlled by a kinetic process in nature. The blue-shift of absorption edge observed in adsorption samples of different kinetic stages (Figure 6) showed that arsenate initially formed a MM complex on TiO_2 surfaces and then continued to react with a nearby bare surface site and became a BB complex. This two-step adsorption mechanism was previously predicted by DFT dynamic calculation in a related study.[5] However, the influence of kinetics on real equilibrium adsorption state had not been considered in conventional adsorption thermodynamic theories until metastable equilibrium adsorption (MEA) theory was proposed.[27]

For a given adsorption reaction under fixed thermodynamic conditions, a polyhedral adsorbate molecule is normally ended in various microscopic adsorption states on solid surface rather than a unique equilibrium structure when adsorption reactions reach the final stage.[28−32] One adsorption state has unique geometry, energy, and chemical potential (e.g., BB complex occupies two active surface sites, whereas MM occupies only one). On the basis of this, MEA theory predicts that the real equilibrium adsorption constants are not constant but fundamentally affected by the kinetics or reactant concentration in nature.[25,27] Under fixed thermodynamic conditions, initial reactant concentration and kinetic pathways can fundamentally alter adsorption equilibrium by affecting the final metastable equilibrium adsorption microscopic structures. When thermodynamic parameters (e.g., equilibrium constants) are expressed in terms of the concentration of adsorbate on solid surface, equilibrium adsorption properties can no longer be explained by traditional thermodynamic theories, because different microscopic MEA states that construct the real equilibrium state cannot be counted for both mass and energy by the macroscopic parameters such as adsorption density (mol/m^2). Therefore, traditional thermodynamic theories need to take metastable equilibrium adsorption (MEA) into account in order to accurately describe real equilibrium properties of surface adsorption.

A 0.12−0.23 eV blue-shift of absorption edge from adsorption samples to corresponding desorption samples was observed (Figures 5 and 6), indicating that the proportion of BB to MM complex increased in desorption processes. During the desorption process, arsenate adsorbed in MM mode had priority to be desorbed from TiO_2 surfaces. Meanwhile, as the surface coverage decreased, some arsenate of MM mode could further react with the nearby newly exposed site to form more stable (or more irreversible) BB complex.

3.4. XANES Interpretation of C_0 Effect. The 0.29 eV blue-shift of absorption edge from one-batch kinetic sample A_5 to three-batch kinetic sample A_{11} (Figure 6) provided an XANES experimental interpretation of why the three-batch adsorption isotherm was lower than the one-batch isotherm (i.e., C_0 effect; see Figures 1 and 2 in ref 7) in the As(V)−TiO_2 adsorption system. In the three-batch adsorption experiment, the initial arsenate concentration in each batch was one-third of that in the one-batch conventional experiment. Under this condition, more MM adsorbed arsenate formed in the first two additions can potentially transfer to BB surface complex due to the low

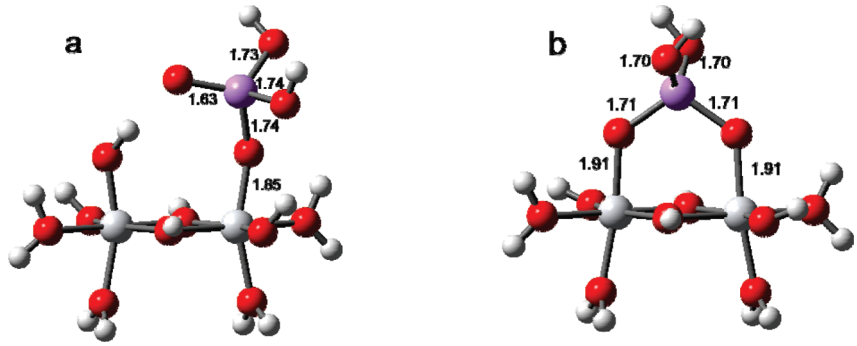

Figure 4. The geometry of Ti−AsO_4 surface complexes calculated using density functional theory: (a) MM and (b) BB. Purple, red, big gray, and small gray circles denote As, O, Ti, and H atoms, respectively. Distances are shown in angstroms.

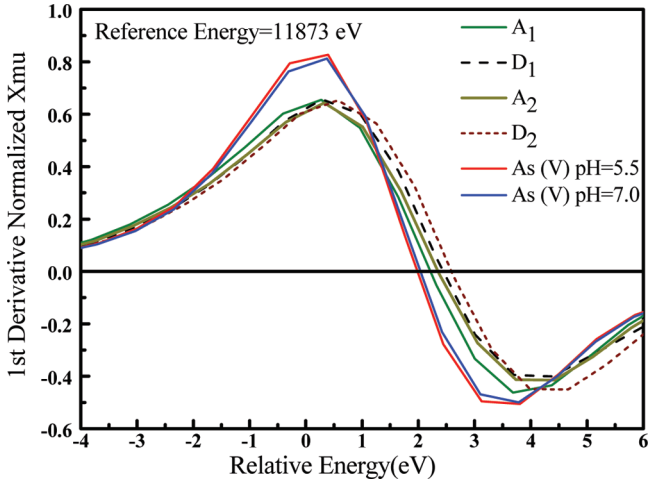

Figure 5. The first derivative As(V) K-edge XANES spectra of one-batch (A_1 and D_1) and three-batch (A_2 and D_2) isotherm adsorption (A)/desorption (D) samples.

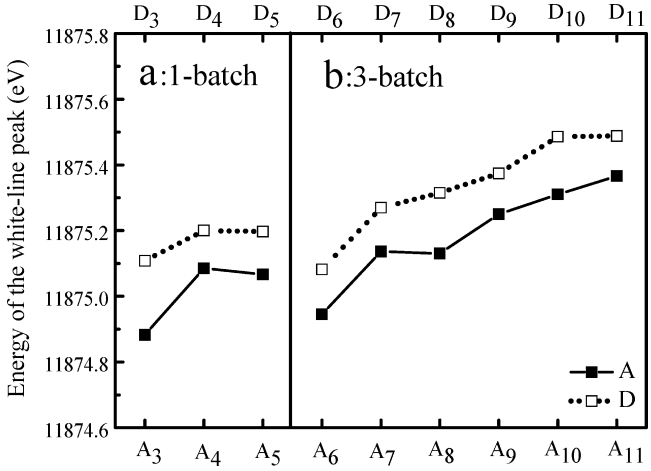

Figure 6. The change of absorption edge of one-batch (a) and three-batch (b) kinetic adsorption/desorption samples.

surface coverage and sufficient surface site, making the final adsorption density decreased because BB mode occupied more surface area than MM mode. Thus, by affecting the transform from MM to BB mode, reaction kinetic pathways or reactant concentration can affect the proportion between different MEA states (i.e., MM:BB ratio in this system) in the real equilibrium adsorption state.

The XANES fingerprint characteristics (Figures 5 and 6) indicated that the real equilibrium adsorption state of arsenate onto Ti-(hydr)oxide was essentially controlled by adsorption kinetic process. Under fixed thermodynamic conditions, the real adsorption state at the solid−liquid interface may vary with reaction kinetic pathways. Traditional adsorption thermodynamic theories need to be further developed by taking MEA into account in order to accurately describe real equilibrium properties of surface adsorption.

3.5. Complementarity of XANES and EXAFS for Structural Assignment. EXAFS can give local structure information around an absorber, i.e. coordination number (CN) and atomic distance (R). Ratio of CN was used as an index to approximate the change of surface complexation mode.[33] However, this approach needs to be further developed due to the detection limitation of EXAFS to coordination number and the artificial error in the EXAFS fitting process. XANES had a much higher sensitivity than EXAFS, which was based on the original spectral data, and had little artificial error in modeling. The combination of EXAFS (geometrical structure prediction) and XANES (electronic fingerprinting analysis) could provide a more accurate estimation for surface structural assignment and surface complexation characteristics.

4. Conclusion

A structural analysis method combining XANES technique with DFT calculation was developed and applied to investigate the bonding mode and structural evolution of arsenate on TiO_2 surfaces. The blue-shift of As(V) K-absorption edge observed in kinetic adsorption samples suggested a structural evolution from monodentate mononuclear to bidentate binuclear adsorption mode during the adsorption kinetic process. The extent of transformation was controlled by reaction kinetic pathway and surface coverage. By affecting the proportion between different MEA states (MM:BB), kinetic pathways or initial concentration of reactants can fundamentally affect real equilibrium adsorption state. The spectral shift of XANES absorption edge provided direct and quantitative information in studying solid−liquid interface adsorption.

Acknowledgment. The study was supported by NNSF of China (20777090, 20621703) and the Hundred Talent Program of the Chinese Academy of Science. We thank Beijing Synchrotron Radiation Facility (BSRF, China) for providing the beam time and Tiandou Hu and Yaning Xie for help in XANES analysis.

References and Notes

(1) Khare, N.; Martin, J. D.; Hesterberg, D. *Geochim. Cosmochim. Acta* **2007**, *71*, 4405.
(2) Ankudinov, A. L.; Ravel, B.; Rehr, J. J.; Conradson, S. D. *Phys. Rev. B* **1998**, *58*, 7565.
(3) Moniek, T.; Jerome, M.; Gillian, R.; John, E. *AIP Conf. Proc.* **2007**, *882*, 699.

(4) Waychunas, G. A.; Fuller, C. C.; Davis, J. A.; Rehr, J. J. *Geochim. Cosmochim. Acta* **2003**, *67*, 1031.
(5) Zhang, M. Y.; He, G. Z.; Pan, G. *J. Colloid Interface Sci.* **2009**, *338*, 284.
(6) He, G. Z.; Pan, G.; Zhang, M. Y. *J. Phys. Chem. C* **2009**, submitted.
(7) Pan, G.; Zhang, M. Y.; He, G. Z. *Environ. Sci. Technol.* **2009**, submitted.
(8) Pena, M.; Meng, X. G.; Korfiatis, G. P.; Jing, C. Y. *Environ. Sci. Technol.* **2006**, *40*, 1257.
(9) Grossl, P. R.; Eick, M.; Sparks, D. L.; Goldberg, S.; Ainsworth, C. C. *Environ. Sci. Technol.* **1997**, *31*, 321.
(10) Ladeira, A. C. Q.; Ciminelli, V. S. T.; Duarte, H. A.; Alves, M. C. M.; Ramos, A. Y. *Geochim. Cosmochim. Acta* **2001**, *65*, 1211.
(11) Sherman, D. M.; Randall, S. R. *Geochim. Cosmochim. Acta* **2003**, *67*, 4223.
(12) Zabinsky, S. I.; Rehr, J. J.; Ankudinov, A.; Albers, R. C.; Eller, M. J. *Phys. Rev. B* **1995**, *52*, 2995.
(13) Ankudinov, A. L. *FEFF8, version 8.20*; the FEFF Project, Department of Physics, University of Washington, 2002.
(14) Lazzeri, M.; Vittadini, A.; Selloni, A. *Phys. Rev. B* **2001**, 63.
(15) Vittadini, A.; Selloni, A.; Rotzinger, F. P.; Gratzel, M. *Phys. Rev. Lett.* **1998**, *81*, 2954.
(16) Homann, T.; Bredow, T.; Jug, K. *Surf. Sci.* **2004**, *555*, 135.
(17) Beltran, A.; Sambrano, J. R.; Calatayud, M.; Sensato, F. R.; Andres, J. *Surf. Sci.* **2001**, *490*, 116.
(18) Hu, Z.; Turner, C. H. *J. Am. Chem. Soc.* **2007**, *129*, 3863.
(19) Paul, K. W.; Borda, M. J.; Kubicki, J. D.; Sparks, D. L. *Langmuir* **2005**, *21*, 11071.
(20) Zhang, N. L.; Blowers, P.; Farrell, J. *Environ. Sci. Technol.* **2005**, *39*, 4816.
(21) Grafe, M.; Sparks, D. L. *Geochim. Cosmochim. Acta* **2005**, *69*, 4573.
(22) Frisch, M. J.; et al. *Gaussian 03, revision C.01wis2*; Gaussian, Inc.: Wallingford, CT, 2004.
(23) Ranea, V. A.; Carmichael, I.; Schneider, W. F. *J. Phys. Chem. C* **2009**, *113*, 2149.
(24) Sun, Q.; Altarawneh, M. N.; Dlugogorski, B. Z.; Kennedy, E. M.; Mackie, J. C. *Environ. Sci. Technol.* **2007**, *41*, 5708.
(25) Pan, G.; Liss, P. S. *J. Colloid Interface Sci.* **1998**, *201*, 77.
(26) Ressler, T. *J. Synchotr. Radiat.* **1998**, *5*, 118.
(27) Pan, G.; Liss, P. S. *J. Colloid Interface Sci.* **1998**, *201*, 71.
(28) Fendorf, S.; Eick, M. J.; Grossl, P.; Sparks, D. L. *Environ. Sci. Technol.* **1997**, *31*, 315.
(29) Li, W.; Pan, G.; Zhang, M. Y.; Zhao, D. Y.; Yang, Y. H.; Chen, H.; He, G. Z. *J. Colloid Interface Sci.* **2008**, *319*, 385.
(30) Manning, B. A.; Hunt, M. L.; Amrhein, C.; Yarmoff, J. A. *Environ. Sci. Technol.* **2002**, *36*, 5455.
(31) Morin, G.; Ona-Nguema, G.; Wang, Y. H.; Menguy, N.; Juillot, F.; Proux, O.; Guyot, F.; Calas, G.; Brown, G. E. *Environ. Sci. Technol.* **2008**, *42*, 2361.
(32) Pan, G.; Qin, Y. W.; Li, X. L.; Hu, T. D.; Wu, Z. Y.; Xie, Y. N. *J. Colloid Interface Sci.* **2004**, *271*, 28.
(33) Li, X. L.; Pan, G.; Qin, Y. W.; Hu, T. D.; Wu, Z. Y.; Xie, Y. N. *J. Colloid Interface Sci.* **2004**, *271*, 35.

JP9044918